International Journal of Engineering Research and Technology.
ISSN 0974-3154 Volume 11, Number 3 (2018), pp. 383-402

http://www.irphouse.com

The Effect of Upper Tank Surface Property on Solar Chimney Power Plant Performance

Mohammed K.Khashan[1], Riyad Jassim Tilefih[2] and Amjed Al-Khateeb[1]

[1] Asst. Lecturer, Najaf Technical Institute, Al-Furat Al-Awsat Technical University 31001 Al-Najaf, Iraq, Department of Aeronautical Technologies,

[2] Lecturer, Najaf Technical Institute, Al-Furat Al-Awsat Technical University 31001 Al-Najaf, Iraq, Department of Aeronautical Technologies.

Abstract

The solar chimney power plants consist of three essential elements, glass roof collector, chimney (tower) and wind turbine. The output power of the system depends on the input velocity to wind turbine. A water tank as thermal storage system was used to enable the system to work at whole the day i.e. 24 hours. The effect of upper tank surface as opaque/transparent property type was studied in the present study. A numerical simulation to investigate the performance of solar chimney power plant was implemented. A small scale model of solar chimney power plant was modelled by using FLUENT software. To solve the governing equations of conservation of mass, momentum, energy, Do- intensity, k and ϵ equations the finite volume method was adopted by FLUENT software to model and analyze such system. The results showed that the property of upper tank surface has an effect on the performance parameters. Using opaque surface will improve system energy gain by 58.75 % of tank surface with transparent property.

Keywords: Solar chimney, Numerical simulation, surface property, Performance parameters.

INTRODUCTION

A solar chimney power plant is a technology that uses solar energy to produce an artificial wind to generate electricity. Solar chimney power plants consist of three essential elements, circular glass roof solar collector (Air heating device), chimney or Tower (Power Generating Component) and wind turbine [1]. Air enters the collector from its periphery and is heated under the collector by heat emitted from glass roof

and absorbing plate. It moves with a radial direction forward toward collector center where chimney base is. The temperature differential between the cool air at the top and the heated air at the bottom creates what is known as "the chimney effect or stack effect" results in a buoyancy force that drives the flow upward and out of the tower. A turbine installed at the base of the tower (for easier access and maintenance) used to extract the available power of flow and converting it to mechanical power (shaft work). Finally, a generator attached to the turbine provides electrical power [2]. Fig (1) shows a schematic layout of solar chimney power plant which illustrates the principle of operation.The geometric parameters of chimney height, collector and base area were investigated by **Ali K. Al-Abadi** [3].The influence of quality collector roof glass and various types of soil on the performance of a large scale solar chimney power plant were studied by **J.P. Pretorius et al.**,[4]. By using numerical analysis based on the (Finite Difference Technique) **H. H. Al-Kayiem et al.,**[5] studied effects of geometries variations (collector covers orientation and the chimney configuration) on the performance of the system. **E. BACHAROUDIS et al.,**[6] use the control volume method to solve the governing elliptic equations for two-dimensional domain to investigate the thermo fluid phenomena occurring inside solar chimneys. **Sh. Khoshmanesh** [7] used FLUENT software to study the variation of velocity with five parameters of the systems which is Absorber Diameter (D_p), Roof glass angle (β), Entrance height (h), Tower's Height (h_t) and Tower's Diameter (D_t). **Atit Koonsrisuk et al**.,[8] used computational fluid dynamic technology (CFD) to investigate the changes in flow kinetic energy caused by the variation of tower flow area with height. The geometry of the major components of the Solar Chimney Power Plant, (solar air collector, chimney tower, and wind turbine) were studied and optimized by **Sandeep K. Patel et al.,**[9].

The present study investigates the effect of property of upper tank surface on the performance parameters of solar chimney power plant were modelled and simulated. Each one differs in upper tank surface property of being opaque or transparent.

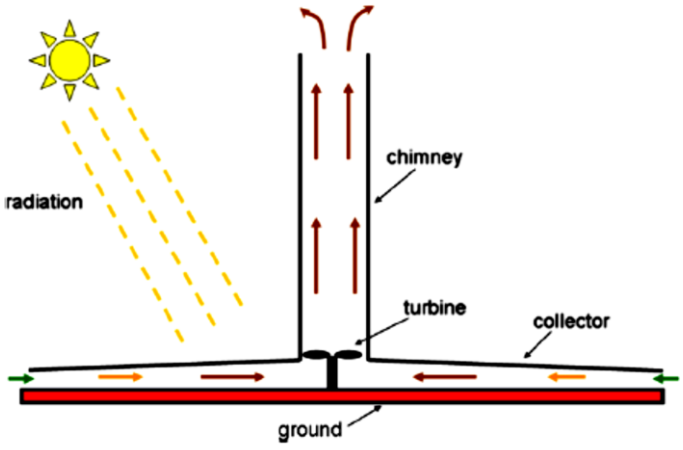

Figure (1): *schematic layout of solar chimney power plant.*

NUMERICAL SIMULATION

Physical model

The Manzanares pilot plant 1:100 scaled model was selected as the physical model to verify the numerical method. The computational domain, is divided into the following zones: the collector, absorbing plate, chimney, and airflow. Fig. (2) shows the power plant scale model and its dimensions.

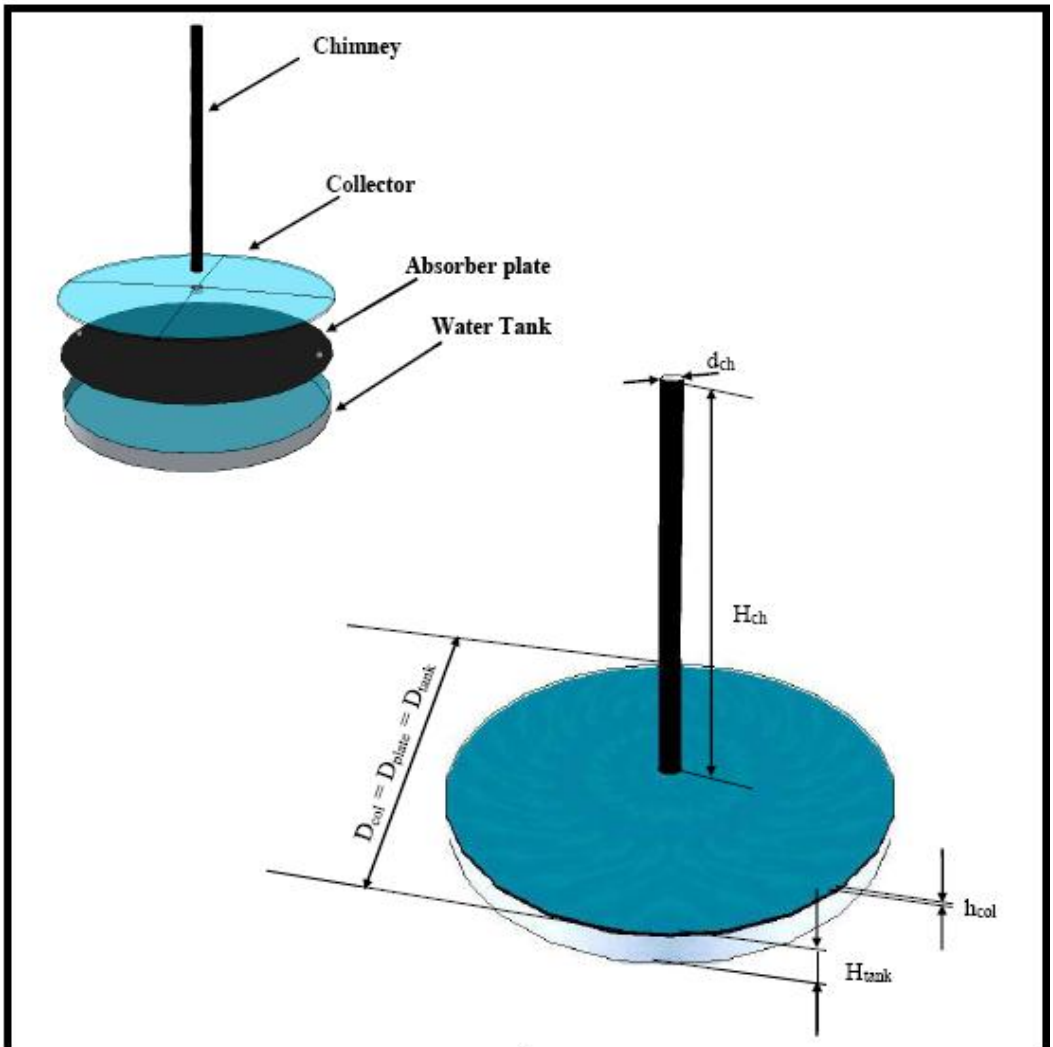

Chimney height (H_{ch})	1.95 m
Collector gap (h_{col})	0.019m
Tank height (H_{tank})	0.15m
Chimney diameter (d_{ch})	0.1m
Collector diameter (D_{col})	2.24 m
Absorbing plate diameter (D_{plate})	2.24 m
Tank diameter (D_{tank})	2.24 m

Figure (2): *power plant scale model and its dimensions.*

Mesh Generation

GAMBIT 2.2.30 software was used for grid generation. The computational domain was discretized using the Triangular/ tetrahedral meshes. The Tetrahedral grid used ensures that the results obtained are of the highest quality and accuracy. Meshing for solar chimney with straight and curved junction are shown in Fig. (3). A grid independence test was done using three different grid sizes of 805,624, 2,306,534and 2,684,867 nodes respectively. The judging criterion was the mass flow rate. The mass flow rates obtained were 0.0047, 0.01381and 0.01365 kg/s. The mass flow rate obtained at 2,306,534 and 2,684,867 nodes grid size showed very little difference which was of the order of 1.15%. So having a very fine mesh would not have been beneficial as it would have prolonged the simulation time and for this reason, a grid size of 2,306,534 nodes was chosen for all the simulations.

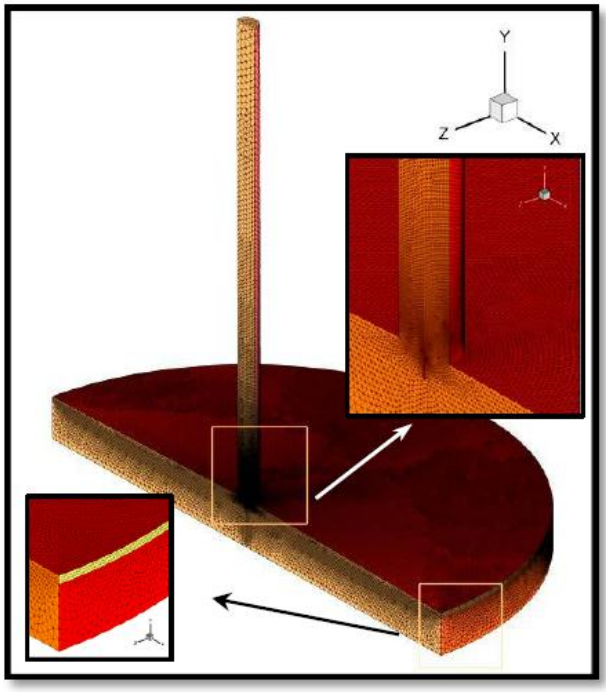

Figure (3): *Meshing of solar chimney physical model.*

Assumption.

In the present study, the flow characteristics are assumed to be as follows,

1. Steady flow.
2. Three dimensional.
3. The working fluid is air and behaves as an ideal gas.
4. Incompressible fluid.
5. Turbulent flow.
6. Newtonian fluid.

MODELLING

All simulations in this study was carried out using the finite volume-based solver FLUENT 6.3.26. Steady state analysis was chosen. The working fluid used was air which was modelled as an ideal gas. The entire model was built from the origin and extended in the positive y-direction. The buoyancy model was activated by specifying the gravity of -9.81m/s^2 in the y-direction which represented real life flow. The reference pressure used was101325 Pascal. Heat transfer in the solar chimney power plant system involves all three modes: conduction, convection, and radiation. In simulating the flow in solar chimney power plant, computations using models that only focus on conduction or convection are the simplest, whereas those involving buoyancy-driven flow and radiation models are more complex. Radiation heat transfer mainly occurs in the collector, which is covered by different types of semi-transparent materials such as glass or plastic. The cover materials are nearly transparent for incident solar radiation but partly opaque for infrared radiation from the ground. In the present simulations, the discrete ordinate (DO) radiation model was adopted to solve the radiative transfer equation for the following reasons: (1) only the DO model can be used to model semi-transparent walls of various types, (2) only the DO model can be used to compute non-gray radiation using a gray band model, (3) the DO model can work well across a full range of optical thicknesses, (4) Computational cost is moderate for typical angular discretization and (5) memory requirements are modest. The (DO) Irradiation model used to applying a solar load directly to the DO model (the irradiation flux is applied directly to semi-transparent walls) that specified as a boundary condition, and the radiative heat transfer is derived from the solution of the DO radiative transfer equation. Solar radiation is modelled using the sun's position vector and illumination parameters, which can be specified by users or by a solar calculator utility provided by FLUENT. Solar load is available for 3-D simulation only and can be used to model steady and unsteady flows. Flow in solar chimney power plant is a kind of buoyancy-driven flow. The strength of the buoyancy-induced flow is measured by the Rayleigh number. Rayleigh number less than 10^7 indicate a buoyancy-induced laminar flow, with transition to turbulence occurring over the range of $10^7 <$ Ra $< 10^{11}$. The Rayleigh number for solar chimney scale model is greater than 10^8 that indicates a buoyancy-induced turbulent flow. Therefore, the k-ϵ turbulence model was selected to describe the airflow inside the system. The Boussinesq model was adopted in this simulation. This model treats density as a constant value in all solved equations, except for the buoyancy term in the momentum equation.

$$(\rho - \rho_\infty)\mathrm{g} \approx - \rho_\infty \beta (T - T_\infty)\mathrm{g}$$

Faster convergence can be achieved by using the Boussinesq model than by setting air density as a function of temperature. The basic equations that describe the movement of the flow are:-

Conservation of Mass (Continuity).

$$\frac{\partial u}{\partial x}+\frac{\partial v}{\partial y}+\frac{\partial w}{\partial z}=0 \quad \text{..... (1)}$$

Navier-Stokes Equations (Momentum).

$$\frac{\partial(\rho uu)}{\partial x}+\frac{\partial(\rho vu)}{\partial y}+\frac{\partial(\rho wu)}{\partial z}=-\frac{\partial p}{\partial x}+\mu[\frac{\partial^2 u}{\partial x^2}+\frac{\partial^2 u}{\partial y^2}+\frac{\partial^2 u}{\partial z^2} \text{ .....} \quad (2)$$

$$\frac{\partial(\rho uv)}{\partial x}+\frac{\partial(\rho vv)}{\partial y}+\frac{\partial(\rho wv)}{\partial z}=-\frac{\partial p}{\partial y}+\mu\left[\frac{\partial^2 v}{\partial x^2}+\frac{\partial^2 v}{\partial y^2}+\frac{\partial^2 v}{\partial z^2}\right]+S_{bj} \text{ .....} \quad (3)$$

$$\frac{\partial(\rho uw)}{\partial x}+\frac{\partial(\rho vw)}{\partial y}+\frac{\partial(\rho ww)}{\partial z}=-\frac{\partial p}{\partial z}+\mu[\frac{\partial^2 w}{\partial x^2}+\frac{\partial^2 w}{\partial y^2}+\frac{\partial^2 w}{\partial z^2}] \text{ .....} \quad (4)$$

Energy Equation.

$$\rho\frac{\partial}{\partial x}(uT)+\rho\frac{\partial}{\partial y}(vT)+\rho\frac{\partial}{\partial z}(wT)=\frac{\partial}{\partial x}\left(\Gamma_{eff.h}\frac{\partial T}{\partial x}\right)+\frac{\partial}{\partial y}\left(\Gamma_{eff.h}\frac{\partial T}{\partial y}\right)+\frac{\partial}{\partial z}\left(\Gamma_{eff.h}\frac{\partial T}{\partial z}\right)+S_T \text{ .....(5)}$$

k-ϵ equations.

Turbulence kinetic energy (k) equation:-

$$\frac{\partial}{\partial x_i}(\rho k u_i)=\frac{\partial}{\partial x_j}\left[\left(\mu+\frac{\mu_t}{\sigma_k}\right)\frac{\partial k}{\partial X_j}\right]+G_K+G_b-\rho\epsilon+S_k \quad \text{.....(6)}$$

The dissipation rate of turbulence energy (ϵ) equation:-

$$\frac{\partial}{\partial x_i}(\rho\epsilon u_i)=\frac{\partial}{\partial x_j}\left[\left(\mu+\frac{\mu_t}{\sigma_\epsilon}\right)\frac{\partial \epsilon}{\partial X_j}\right]+C_{1\epsilon}\frac{\varepsilon}{k}(G_k+C_{3\epsilon}G_b)-C_{2\epsilon}\rho\frac{\epsilon^2}{k}+S_\epsilon \text{ .....} \quad (7)$$

Where. $\quad G_k=-\rho\overline{u_i'u_j'}\frac{\partial u_j}{\partial x_i}$; $\quad G_b=\beta g_i\frac{\mu_t}{Pr_t}\frac{\partial T}{\partial x_i}$

($C_{1\epsilon}, C_{2\epsilon}, C_\mu, \sigma_k and\ \sigma_\epsilon$) are the model constants and have default values illustrated in Table (1).

Table (1): *The $k-\epsilon$ Turbulence Model Constants*.

$C_{1\epsilon}$	$C_{2\epsilon}$	C_μ	σ_k	σ_ϵ
1.44	1.92	0.09	1	1.3

Do-intensity equation.

$$\nabla.(I(\vec{r},\vec{s})\vec{s}) + (\alpha+\sigma_s)I(\vec{r},\vec{s}) = \alpha n^2 \frac{\sigma T^4}{\pi} + \frac{\sigma_s}{4\pi}\int_0^{4\pi} I(\vec{r},\vec{s}')\Phi(\vec{s}.\vec{s}')\,d\Omega' \ldots(8)$$

Boundary conditions.

Boundary conditions specify the flow and thermal variables on the boundaries of the physical model. The boundary conditions applied in this present work are those shown in Fig. (4) and Table (2). Tables (3) and (4) show the momentum and turbulence boundary conditions for the whole parameters of the Solar Chimney Power Plant model in details. Tables (5) and (6) show the radiation boundary conditions and thermal condition in details.

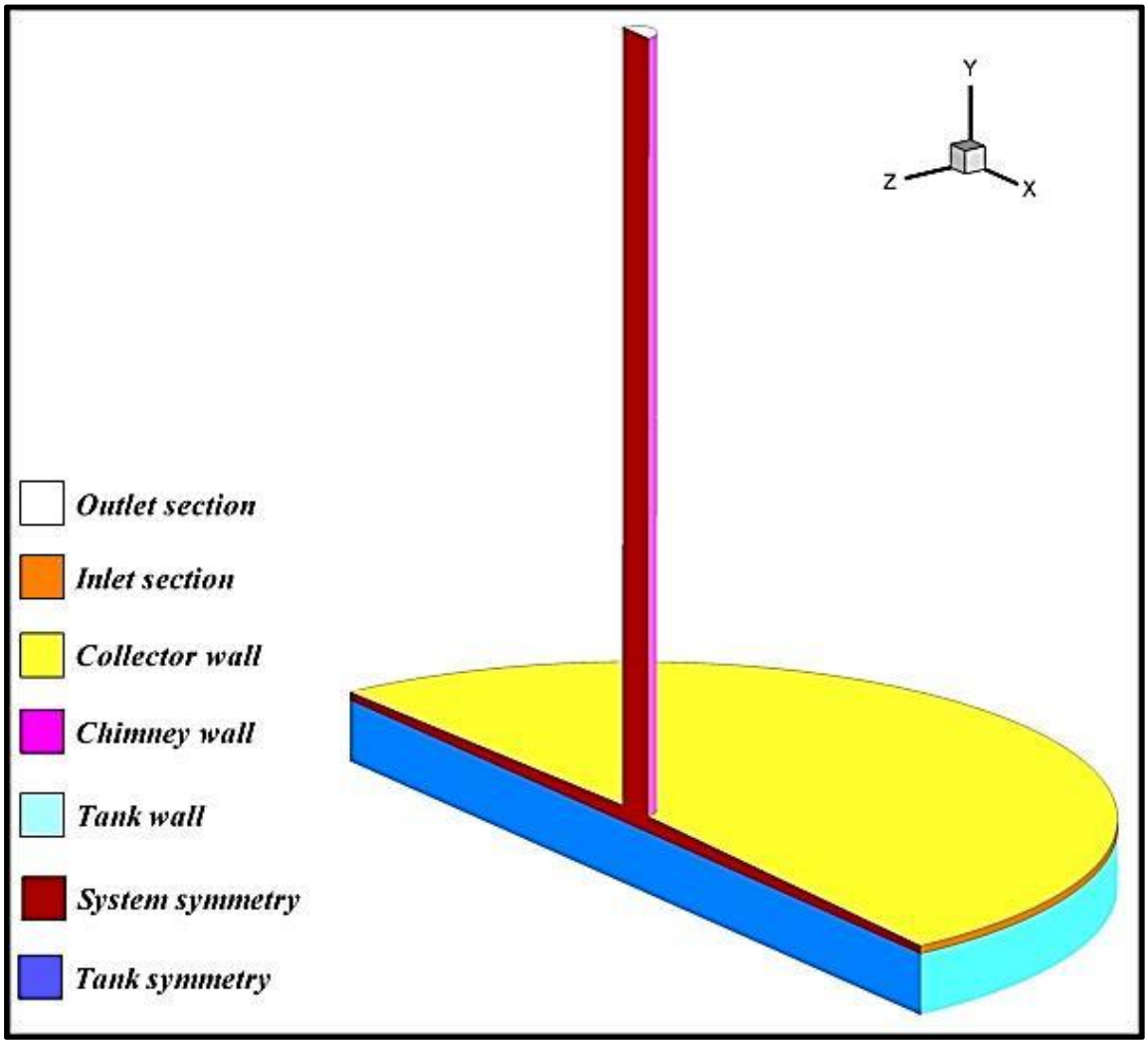

Figure (4): *Boundary conditions of the solar chimney model.*

Table (2): *Boundary Conditions Types of solar chimney model.*

Zone	***Type***
Chimney	*Wall*
Collector	*Wall*
Absorbing plate	*Wall*
Side system wall	*Symmetry*
Periphery tank surface	*Wall*
Lower tank surface	*Wall*
Side tank wall	*Symmetry*
Inlet section	*Pressure inlet*
Outlet section	*Pressure outlet*
Air	*Fluid*
Water	*Fluid*

Table (3): *Momentum boundary conditions.*

Part	***Type***	***Momentum Conditions***	
		Wall Motion	***Shear Condition***
Chimney	*Wall*	*Stationary*	*No Slipping*
Collector	*Wall*	*Stationary*	*No Slipping*
Absorbing plate	*Wall*	*Stationary*	*No Slipping*
Side tank wall	*Wall*	*Stationary*	*No Slipping*
Lower tank wall	*Wall*	*Stationary*	*No Slipping*
Input section	*Pressure inlet*	*- Gauge Pressure = (0 Pascal), [constant].* *- Flow direction specification Method : (Normal to Boundary).*	
Outlet section	*Pressure Outlet*	*- Gauge Pressure = (0 Pascal), [constant].* *- Backflow Direction specification Method: (Normal to Boundary).*	

Table (4): *Turbulence boundary conditions.*

Part	Type	Momentum Conditions
Input section	*Pressure inlet*	*- Gauge pressure = (0 Pascal), [constant].*
		- Turbulent Intensity = 10%
		- Hydraulic diameter = 0.038m
Outlet section	*Pressure outlet*	*- Gauge pressure = (0 Pascal), [constant].*
		- Turbulent Intensity = 10%
		- Hydraulic diameter = 0.1

Table (5): *Radiation boundary conditions.*

Part	Radiation Boundary Conditions
Chimney	*Opaque or Semi-transparent*
Collector	*Semi-transparent (I = 807.56 W/m^2)*
Absorbing plate	*Opaque or Semi-transparent*
Input section	*External black body temperature = Boundary temperature*
Outlet section	*External black body temperature = Boundary temperature*

Table (6): *Thermal boundary conditions.*

Part	Type	Thermal Conditions
Chimney	*Mixed*	*-Heat transfer coefficient = 8.29 W/m2-K* *- Free stream temperature = T_∞ = 46 °C* *- External emissivity = 0.86* *- External radiation Temperature = 0.0552 $T_\infty^{1.5}$* *- Wall Thickness = 0.003 m.* *- Heat generation Rate = 0 (W/m3).*
Collector	*Mixed*	*-Heat transfer coefficient = 8.29 W/m2-K* *- Free stream temperature = T_∞ = 46 °C* *- External emissivity = 0.87* *- External radiation temperature = 0.0552 $T_\infty^{1.5}$* *- Wall Thickness = 0.004 m.* *- Heat generation Rate = 0 (W/m3).*

Part	***Type***	***Thermal Conditions***
Upper tank wall (Absorber plate)	*Coupled*	*- Wall Thickness = 0.0015 (m).* *- Heat generation Rate = 0 (W/m^3).*
Side tank wall	*Constant temperature*	*-Temperature = T_∞ = 46 °C* *- Wall Thickness = 0.04 (m).* *- Heat generation Rate = 0 (W/m3).*
Lower tank wall	*Constant temperature*	*-Temperature = T_∞ = 46 °C* *- Wall Thickness = 0.04 (m).* *- Heat generation Rate = 0 (W/m3).*
Input section	*Pressure inlet*	*-Total temperature = 46 °C*
Outlet section	*Pressure outlet*	*-Backflow Total Temperature = 46 °C*

Solution method.

The governing equations are solved on a staggered grid and the coupling between the momentum and continuity equations through pressure is based on the simple (Semi Implicit Pressure Linked Equation) scheme. The second order, upwind scheme is applied for convective terms of the momentum and energy transport equations, whereas pressure is discretised using the PRESTO! (PREssure STaggering Option) scheme. To ensure numerical stability, the discretized equations are solved by iteration with under-relaxation factors of 0.3 for pressure, 0.7 for momentum, 0.8 for Turbulent kinetic energy, turbulent dissipation rate and 1 for density, body force, turbulent viscosity, Do-Intensity and energy. Solution convergence is controlled by setting the convergence criterion (residual) to 10^{-3} for each equation except for the energy and Do-Intensity equations, which is set to 10^{-6}. All results reported in this paper are obtained using a double precision solver.

Calculations.

1- *Air mass flow rate* can be calculate as follow:-

$$\dot{m}_a = \rho_a \,.\, V_a \,.\, A_{ch} \quad \text{……..…… (9)}$$

2- *Available power* can be calculate as follow:-

$$P_{available} = 0.5\, \rho_a \,.\, A_{ch} . V_a^3 \quad \text{……..…… (10)}$$

3- *Energy gain can be calculated as follow:-*

$$Q_{gain} = m_w . c_p . (T_{final} - T_{initial}). \quad \text{……..…….. (11)}$$

4- *Energy loss can be calculated as follow:-*

$$Q_{loss} = m_w . c_p . (T_{inital} - T_{final}). \quad \text{……..…… (12)}$$

RESULTS AND DISCUSSION

To show the effect of entrance geometry type junction on the performance of solar chimney power plant, the results of 4 tests are presented graphically in a form of performance curves from to predict the performance of plant. The FLUENT data results for four tests are shows in Fig. (13) to (19).

Performance Parameters.

1- Airflow Temperature.

Figure (5) shows the relation between air flow temperature and non-dimensional flow path from collector inlet to chimney outlet. It shows two curves one of them represents airflow temperature distribution in case of upper tank surface opaque and the other for upper tank surface transparent, in spite of both surface are exposed to the same solar radiation and the same incidence angle. The reason for the deference is due to absorbing plate location. The location of absorbing plate in case of opaque upper tank surface is located between two fluids, the air on the upper side and the water on the lower side. The amount of solar radiation that reach to this surface is higher than that reach to the surface under water layer in case of transparent upper tank surface. The absorbing plate is represented in this case by tank base and circumference tank wall. Each curve in this figure has the same behavior where, the airflow temperature increases along the flow path in the collector region and then abrupt dip at chimney base. After that it decreases slowly along the flow path at chimney region. This is because of the increasing airflow temperature at collector region caused by Greenhouse effect and heat transfer from absorber plate. The abrupt dip of airflow temperature at chimney base is caused by the response of abrupt velocity change due to flow area reduction. The decreasing of air flow temperature along the chimney region is due to heat transfer from flowing hot air to the chimney wall.

As can be seen in this Figure, the distribution increases with the time increase, because of effect of change of solar radiation intensity during the day due to the movement of the earth around its axis, as shown in Fig. (6). The variation of solar radiation intensity causes a change in the geographical location of the station relative to the sun. the increase of solar radiation will serve to increase the temperature of air particles.

2- Absorbing Plate Temperature.

Figure (7) shows the relation between plate surface temperature and non-dimensional surface path from surface circumference to surface center. It shows that, the upper tank surface temperature increases along surface from circumference towards the center to record maximum value at mid surface. Then it decreases towards surface center. This behavior is because, when air enters the system from collector gap will decrease the surface temperature because of its cooling effect. This effect extends from entrance region surface circumference to mid surface. After that the surface

temperature will decrease at center due to chimney suction. As can be seen in this Figure, it consists of 10 curves of surface temperature distribution. The red one represents the upper tank surface treated as an absorber plate. The blue one represents the upper tank surface treated as transparent surface.

When upper tank surface is treated as an absorber plate, the plate is located between two fluids, air on top and water at the bottom. The black color will absorbs all wavelengths of sunlight. The opaque tank surface heats up quickly after that it begins to loose heat to surrounding. When air enters to the system through collector gap its temperature increases by effect of emitted heat from absorbing plate. The temperature of water under absorbing hot plate increases also due to emitted heat from absorbing plate and this heat is transferred by convection to water near the base of the tank as shown in Fig. (8). It illustrates the relation between distribution of water temperature and non-dimensional path. It shows that the temperature of water record maximum value at water near upper tank surface due to absorbing hot plate effect, and decreases gradually towards tank base.

When upper tank surface is transparent, the tank base and tank circumference wall act as absorber surfaces. Transparent surfaces allow sunlight to pass through them. But The physical nature of the material determines the amount of radiation that passes through. Which, depends on the wavelengths of light falling on material. The glass material allow short wavelength (380 –700) nm of electromagnetic spectrum (i.e. visible light) to pass through it and is opaque and highly non-reflective for long wavelength between (6600-8200)nm. This surface allows certain wavelengths of the electromagnetic spectrum to pass through. Other wavelengths are absorbed or reflected to the medium in which it came from. In this case the lower tank surface represents an absorber plate to absorb solar radiation that pass through collector glass, tank surface and reach water. The solar radiation that strikes the collector glass, decreases due to reflection and absorption effects through collector glass roof. The transmitted beam will suffer the same effect when it pass through tank surface toward tank base. When solar radiation reach water its energy is dissipated due to translucence effect of water. So the amount of heat reach to tank base and circumference wall is lower than the heat that reaches when absorbing plat represents upper tank surface as shown in Fig. (8).

3- Airflow Velocity.

The motive force that move the flow from collector gap to chimney outlet is caused by combined effect of the flow area reduction and amount of heat transfer from the absorber plate along the film to the working fluid (air). Figure (9) shows the relation between airflow velocity and non-dimensional flow path from collector inlet to chimney outlet . It shows that, the airflow velocity increases gradually along the flow path in the collector region and then increases sharply at collector center. After that, along the flow path at chimney region the velocity tends to be stable and then increases slowly near chimney outlet section. This is because the increase of velocity at collector region is due to heat transfer from the absorbing plate to the working

fluid. This will increase the kinetic energy of air particles along the collector passage. The sharp increase of airflow velocity at collector center is caused area reduction. The air flow velocity is inversely proportional with solar collector radius because the solar collector design of the system has air flow direction to the center of the solar collector where chimney inlet section is. The air flow velocity at inlet to the solar collector from circumference (R_c)outer=1.12 m) has minimum value. At the center of the solar collector where chimney exist (R_c) inner = 0.05m) the airflow velocity has maximum value ($V_r \propto 1/R_c$). This agrees well with [10]. The cause of stability of airflow velocity at mid part is due to that the flow is fully developed. The small increase of airflow velocity in chimney region near the outlet section is caused by amount of air temperature rise (ΔT) between ambient and chimney outlet draft. The chimney's outlet draft has a temperature higher than the ambient temperature. That indicates the density inside is lower than ambient, which will accelerate the flow, as can be seen in this figure. It, consists of two curves one of them for upper tank surface with opaque property (the red one), and the other for transparent tank surface (the blue one). In spite of that both surfaces are exposed to the same solar radiation and the same incident angle, but differs in airflow velocity distribution. The reason behind this is the absorber plate location. The location of absorbing plate in case of opaque upper tank surface between two fluids, the air from the upper side and the water from the lower side. The amount of solar radiation that reach to this surface is higher than that reach to the surface when located under water layer in case of transparent upper tank surface. The absorber is represented by tank base and tank circumference wall. The amount of heat that emitted from upper surface which is picked by air particles in case of opaque surface differs from that emitted by transparent surface. This will reduce the flow temperature as a result its density increases compared to flow flowing over opaque surface. This figure also indicates that velocity distribution increases with the time increase, because of variation of solar radiation intensity during the day due to the movement of the earth around its axis.

4- Working Air Mass Flow Rate ($\dot{m}$).

Figure (10) shows the relation between working air mass flow rate Vs time. It shows that the working air mass flow rate increases with time because of increasing in air flow velocity due to solar radiation increase.

5- Flow Available Power ($P_{available}$).

Figure (11) shows the relation between flow available power Vs time. It shows that the flow available power increases with time, because of increasing in working air mass flow rate due to solar radiation increase.

6- Heat Gain(Q_{Gain}) and Heat Lost (Q_{Lost}).

Figure (12) shows the relation between heat gain Vs time. It shows that the heat gain increases with time, due to solar radiation increase. The difference between the two distributions is due to the absorber plate location.
Figures (13) to (19) show the velocity vectors and temperature contours for present case.

CONCLUSIONS

The property of upper tank surface (opaque or transparent) has an effect on the performance parameters. the results showed that

1- The location of absorber plate to be upper tank surface will improve performance parameters of solar chimney system.
2- When periphery and lower tank surface behaves as an absorber plate the performance parameters of solar chimney will deteriorate.
3- Using opaque surface will improve system energy gain by 58.75 % of tank surface with transparent property.

Nomenclature		
Symbol	***Description***	***Unit***
A	*Area*	m^2
a	*Absorption coefficient*	---
$C_{1\varepsilon}$, $C_{2\varepsilon}$, $C_{3\varepsilon}$, C_{μ}	*Turbulence Model Constants*	---
g	*Gravitational Acceleration (9.81)*	m/s^2
G_b	*Generation of turbulence kinetic energy due to buoyancy*	---
G_k	*Generation of turbulence kinetic energy due to the mean velocity gradients*	---
I	*Radiation intensity*	W/m^2
k	*Turbulence Kinetic energy*	---
$\dot{m}$	*Mass Flow Rate*	kg/s
n	*Refractive index*	---
P	*Available Power*	kW
$\vec{r}$	*Position vector*	---
S_{bj}	*Buoyancy source or sink term*	---

$\vec{s}$	*Direction vector*	---
$\vec{s}'$	*Scattering direction vector*	---
S_k, S_ϵ,S_T	*User-defined source terms*	---
T	*Temperature*	^oC
u	*Stream-wise velocity*	*m/s*
v	*Velocity*	*m/s*
v	*Lateral velocity*	*m/s*
w	*Vertical velocity*	*m/s*
x, y, z	*The corresponding Cartesian axis*	---
Greek Symbols		
Symbol	***Description***	***Unit***
∂	*Partial differential operator*	---
β	*Thermal expansion coefficient*	*1/K*
ϵ	*Turbulence energy dissipation rate*	---
μ	*Dynamic viscosity*	*Pa.m*
ρ	*Density*	kg/m^3
σ_k, σ_ε	*Turbulent Prandtl number for K and ε*	---
σ_s	*Scattering coefficient*	---
Φ	*Phase function*	---
Γ	*Diffusion coefficient*	---
Ω'	*Solid angle*	*Degree*
Subscripts		
Subscript	***Description***	
av	*Average (at chimney base)*	
c	*Collector*	
ch	*Chimney*	
eff	*Effective condition*	
i, j, k	*The three coordinate directions*	
t	*Turbulent flow condition, total*	
∞	*Ambient*	

Abbreviations	
Abbreviations	***Description***
CFD	*Computational Fluid Dynamics*
DO	*Discrete Ordinates*
FLUENT	*Fluid And Heat Transfer Code*
GAMBIT	*Geometry And Mesh Building Intelligent Toolkit*
PRESTO!	*Pressure Staggering Option*
SIMPLE	*Simi-Implicit Method For Pressure Linked Equation*
SCPP	*Solar Chimney Power Plant*

REFERENCES

[1] Jeffrey Freidberg, "Solar updraft towers: their role in remote on-site generation", pp 1-31, (2008).

[2] Schlaich Bergermann und partner, "the solar chimney", Structural Consulting Engineers, pp 1-14, (2002).

[3] Ali K. Al-Abadi, Ahmed F. Kridi and Ghassan Fadhil M. Hussain, "Comparison between Simulated and Calculated Power of the Solar Chimney with Black Concrete Base using Ansys Program", Al-Qadisiya Journal For Engineering Sciences, Vol. 3, No. 3, pp. 347-364, (2010).

[4] J.P. Pretorius and D.G. Kröger," Critical evaluation of solar chimney power plant performance", Science Direct, pp. 535-545, (2005).

[5] H. H. Al-Kayiem and Q. A. Al-Nakeeb, "Geometry Alteration Effect on the Performance of a Solar-Wind Power System, International Conference on Energy & Environmental Systems(ICEE), (2006).

[6] E. BACHAROUDIS, M.GR. VRACHOPOULOS, M.K. KOUKOU and A.E. FILIOS," Numerical investigation of the buoyancy-induced flow field and heat transfer inside solar chimneys", International Conference on Energy & Environmental Systems(ICEE), pp. 293-298, (2006).

[7] Sh. Khoshmanesh, " Computer Simulation of Solar Updraft Tower Systems to Describe the Variation of Velocity with Essential Parameters of the Systems ", International Conference on Energy & Environmental Systems(ICEE), pp. 1-5, (2006).

[8] Atit Koonsrisuk and Tawit Chitsomboon,″ Effect of Tower Area Change on the Potential of Solar Tower″, Sustainable Energy and Environment (SEE), pp.1-6, (2006).

[9] Sandeep K. Patel, Deepak Prasad and M. Rafiuddin Ahmed, "Computational studies on the effect of geometric parameters on the performance of a solar

chimney power plant ", Science Direct, pp. 424–431,(2014).

[10] Hussam Abd-Alrazak Falih, " Design study of vertical solar chimney power plant ", M.Sc. Thesis, Al-Nahrain University, Iraq, (2004).

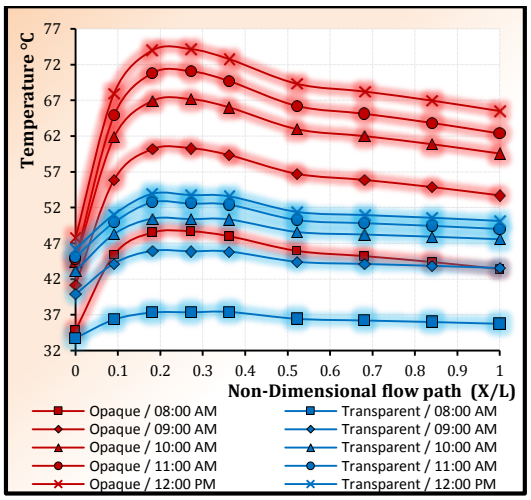

Figure (5): *Air flow temperature distribution for opaque and transparent property of upper tank surface.*

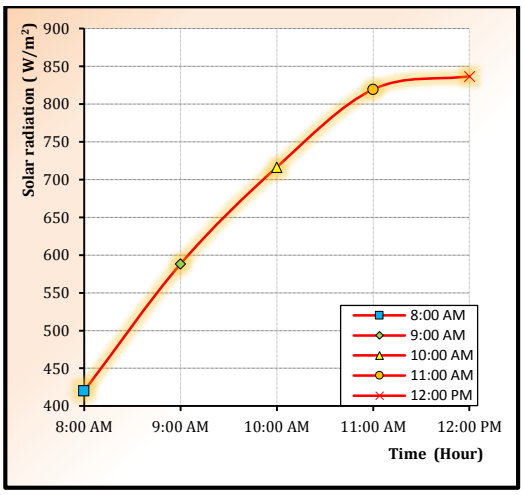

Figure (6): *Distribution of solar radiation Vs time.*

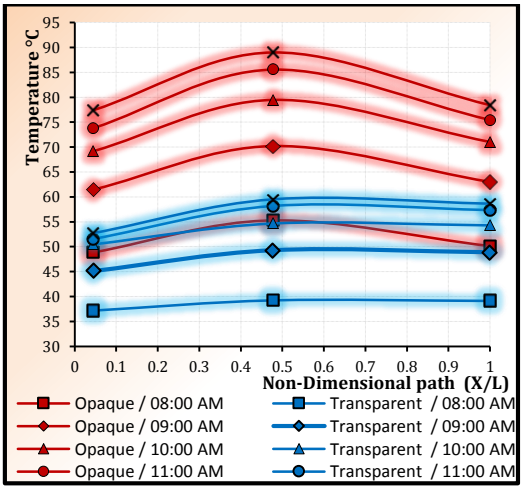

Figure (7): *Surface temperature distribution for opaque and transparent property of upper tank surface.*

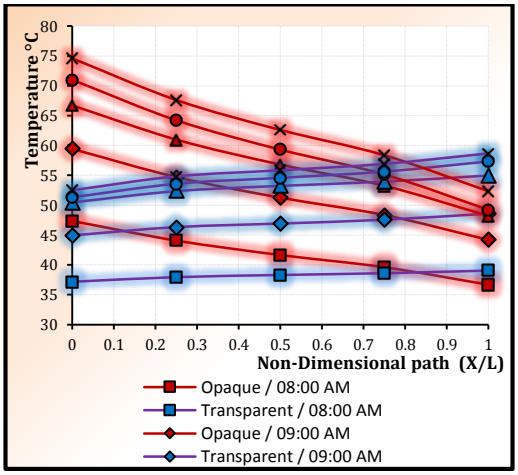

Figure (8): *Water temperature distribution for opaque and transparent property of upper tank surface.*

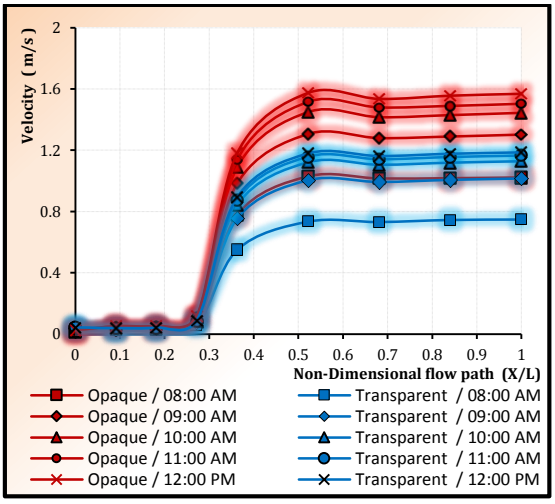

Figure (9): *Velocity distribution along flow path from collector entrance until chimney outlet for both cases..*

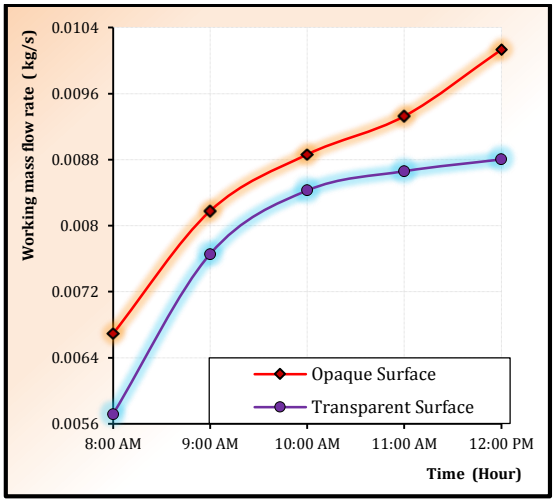

Figure (10): *Theoretical working air mass flow rate Vs time for opaque and transparent property of upper tank surface.*

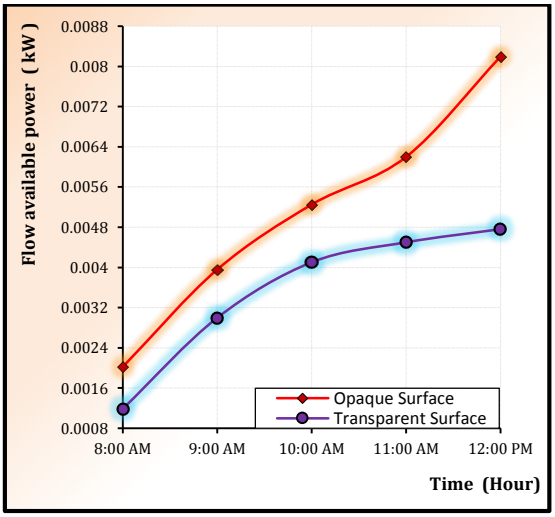

Figure (11): *Theoretical flow available power Vs time for opaque and transparent property of upper tank surface.*

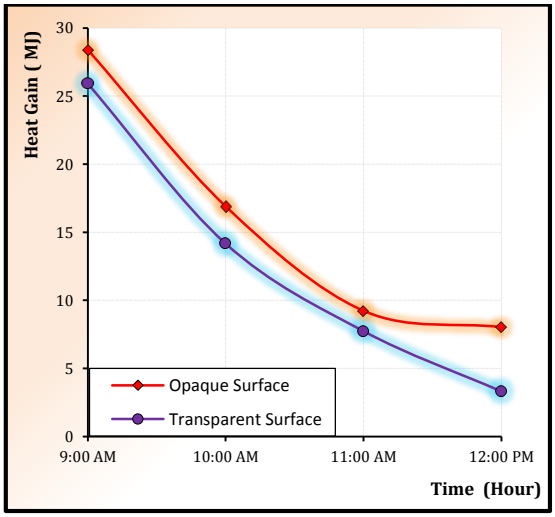

Figure (12): *Theoretical useful heat storage Vs time for opaque and transparent property of upper tank surface.*

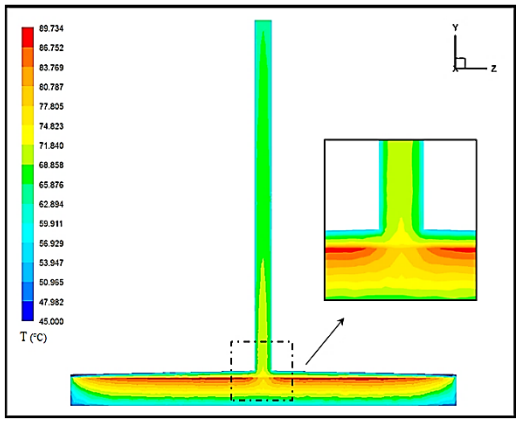

Figure (13): *Temperature's contours of opaque tank surface.*

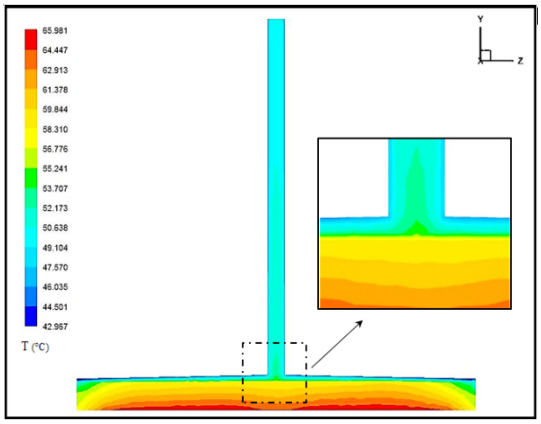

Figure (14): *Temperature's contours of transparent tank surface.*

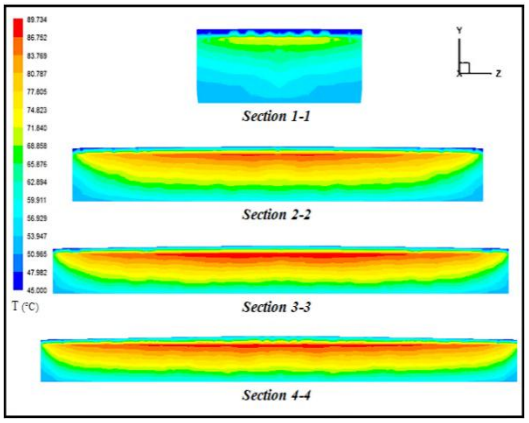

Figure (15): *Temperature contours illustrate temperature stratification for opaque tank surface.*

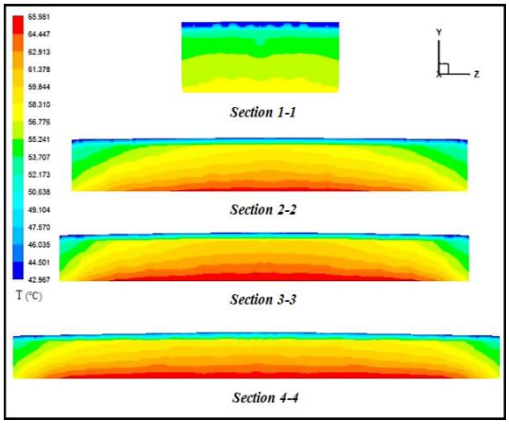

Figure (16): *Temperature contours illustrate temperature stratification for transparent tank surface.*

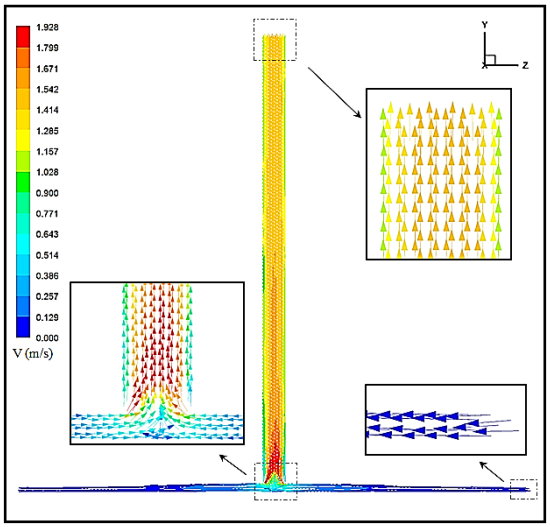

Figure (17): *Velocity vector contour for opaque tank surface.*

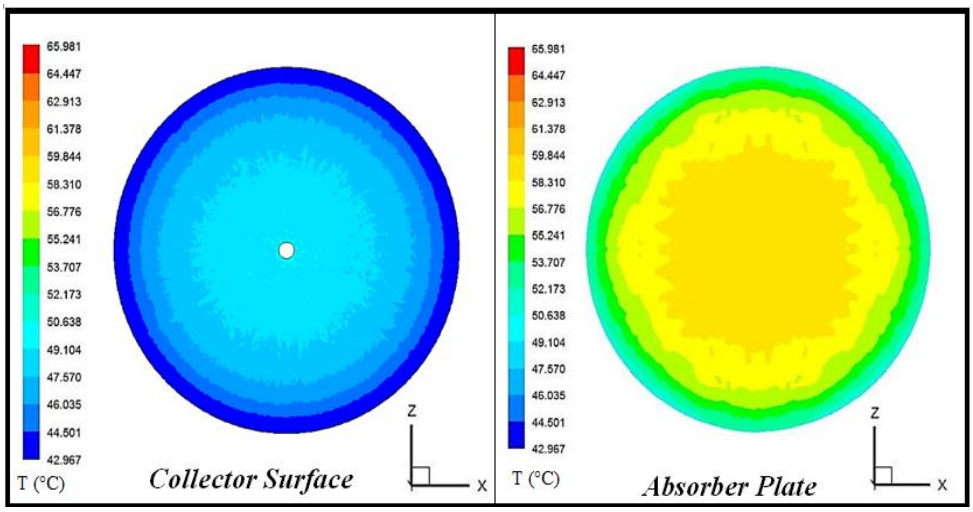

Figure (18): *Temperature's contour of collector and absorber plate for opaque tank surface.*

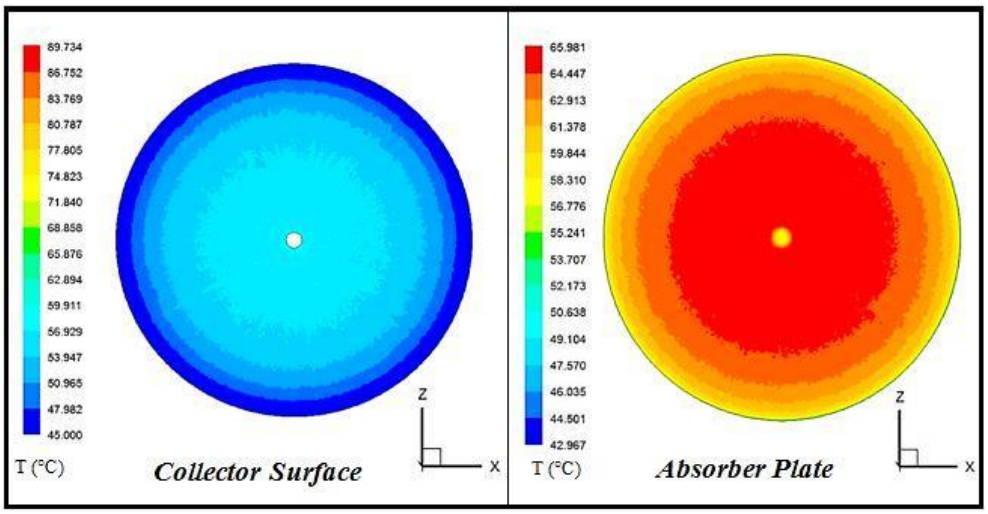

Figure (19): *Temperature's contour of collector and absorber plate for transparent tank surface.*